Available online at www.sciencedirect.com

SciVerse ScienceDirect

Physics Procedia 42 (2013) 58 – 65

Physics Procedia

PNCMI 2012 - Polarized Neutrons for Condensed Matter Investigations 2012

Towards a modelling of USANSPOL intensities from magnetic ribbons

E. Jericha[1], G. Badurek, C. Gösselsberger

Atominstitut, Vienna University of Technology, Stadionallee 2, 1020 Wien, Austria

Abstract

Amorphous magnetic ribbons represent both novel technologically relevant complex samples which are currently in the process of material development for use as magnetic sensors and actuators due to their exceptional magnetostriction properties as well as illustrative examples for developing the technique of ultra-small-angle polarised neutron scattering (USANSPOL) for the study of magnetic microstructure. We present the formalism on which the USANSPOL technique is based and highlight a potential route on which USANSPOL data analysis may be performed. Experimentally obtained scattering patterns are the results of a variety of parameters like material composition and production conditions as well as various environmental conditions, including zero-field environment, the influence of external magnetic field, mechanically induced stress, or a combination of both effects, and in magnetically saturated state. In the case of non-isotropic structures a two-dimensional record of the scattered neutron intensity is essential and more complexity is added by the special features of magnetic neutron scattering and the USANSPOL technique itself. In this work we concentrate on these peculiarities and describe the current experimental status which is driven by the underlying USANSPOL scattering formalism. Recent experimental results are presented to illustrate the phenomenological correspondence to our modelling.

Selection and peer-review under responsibility of the Organizing Committee of the 9th International Workshop on Polarised Neutrons in Condensed Matter Investigations

Keywords: USANSPOL, polarised neutrons, small-angle neutron scattering, amorphous magnets, magnetic ribbons
PACS: 61.05.fg, 61.05.fm, 03.75.Be, 25.40.Dn, 81.40.-z, 75.50.Kj, 75.60.Ch, 75.60.Ej
2010 MSC: 82D40, 65C20

1. Introduction

The technique of ultra-small-angle scattering of polarised neutrons (USANSPOL) aims at the study of the magnetic micro-structure of condensed matter. Thereby we rely on its μrad angular resolution which allows accessing scattering structures in the μm size range, typically a few tenths up to few tens of a micrometre. This is also the size range of magnetic domains in many samples of technological interest. Since USANSPOL is a perfect crystal neutron optics technique, thermal and moderately cold neutrons have to be employed and the corresponding scattering angles range from the resolution limit at a few μrad up to

[1]Email: jericha@ati.ac.at

Selection and peer-review under responsibility of the Organizing Committee of the 9th International Workshop on Polarised Neutrons in Condensed Matter Investigations
doi:10.1016/j.phpro.2013.03.176

about 1 mrad. Additionally, under certain model assumptions the scattered intensity may be extrapolated to zero forward scattering angle. While, in general, an ab initio determination of the magnetic micro-structure without any complementing information is rather difficult, the USANSPOL technique allows us to follow structural evolution under varying external forces. In [1] and [2] we have investigated the micro-structure of magnetic ribbons of technological interest placed in external magnetic fields and subjected to mechanically induced stress having the exceptional magnetostriction properties of some of the ribbons in mind. These samples allow for the observation of a variety of scattering patterns and are therefore ideal for characterisation of the USANSPOL technique and its potential and limitations. Typical dimensions of such ribbons as given by the manufacturing process as well as from the suitability for USANSPOL measurements are widths of few mm to few cm, lengths of 1–10 cm and thicknesses of 10–100 μm. In this work we discuss the underlying formalism which leads to the formation of the measured neutron intensity. This work may be considered as a conceptual extension to [1] and [2] based on recent experiences in USANSPOL data treatment. Instrumental details of the USANSPOL setup can be found in these references.

2. Formal description of the measured neutron intensity

The aim of a USANSPOL measurement is the extraction of the spatial dependence of the average neutron scattering length density $\rho(\mathbf{r}) = N\langle b\rangle(\mathbf{r})$ from the measured neutron intensity. Quantities involved are the local particle density N, the local number of atoms, molecules or formula units per unit volume. In amorphous materials we assume this number to be constant throughout the sample. $\langle b\rangle$ is the average neutron scattering length consisting of a nuclear and a magnetic contribution which may vary with position. The intensity scattered from a particular structure within the sample follows from the Fourier transform of its average scattering length density, $\rho(\mathbf{Q})$, as

$$I(\mathbf{Q}) \propto |\rho(\mathbf{Q})|^2 = (N\langle b(\mathbf{Q})\rangle V)^2 S(\mathbf{Q}) \tag{1}$$

with its scattering function $S(\mathbf{Q})$ and its volume V. Denoting the components of the scattering vector $\mathbf{Q}$, we set Q_x in direction of the incoming neutron beam, and the other two components transversal to that direction, Q_y horizontal and Q_z vertical. In the case of ultra-small-angle neutron scattering Q_x is negligible with respect to the transversal components and the configuration may be described as 2-dimensional. Furthermore the method provides its high resolution only parallel to the reciprocal lattice vector perpendicular to the reflecting crystal planes of the monochromator and analyser crystals while it essentially integrates over the perpendicular scattering direction. In a usual USANS configuration the high resolution is in the horizontal Q_y plane and integration, the so-called *slit height smearing*, is performed along the vertical Q_z axis

$$I(Q_y) \propto \int \mathrm{d}Q_z (N\langle b(Q_y, Q_z)\rangle V)^2 S(Q_y, Q_z) \tag{2}$$

For magnetic scattering the average scattering length depends on the coherent scattering length b_c, the magnetic scattering length $b_m = -\gamma_n r_e S$ with the gyromagnetic ratio $\gamma_n = -1.913$, the classical electron radius $r_e = 2.818$ fm and the effective atomic spin S, the atomic magnetisation $\mathbf{M}$ and the polarisation of the neutron beam $\mathbf{P}$,

$$\langle b(\mathbf{Q})\rangle = b_c + b_m \mathbf{P} \cdot \hat{\mathbf{M}}_\perp(\mathbf{Q}) \tag{3}$$

where the atomic magnetic form factor has been set to unity as applicable in the USANSPOL regime. $\hat{\mathbf{M}}_\perp(\mathbf{Q})$ is a unit vector and points in the direction of the component of the average magnetisation of the scatterer perpendicular to the scattering plane and hence to the scattering vector $\mathbf{Q}$. This dependence on $\mathbf{Q}$ becomes specifically important for slit height smearing. In our current USANSPOL setup the incoming neutron beam is polarised along the z axis and the polarisation may be rotated in the (y, z) plane to an arbitrary angular position before the neutrons hit the sample. Under these conditions $\langle b(\mathbf{Q})\rangle$ is expressed as

$$\langle b(\mathbf{Q})\rangle = \langle b(Q_y, Q_z)\rangle = b_c + b_m[P_y \hat{M}_{\perp y}(Q_y, Q_z) + P_z \hat{M}_{\perp z}(Q_y, Q_z)] \tag{4}$$

and with the components of the average magnetisation unit vector $\hat{\mathbf{M}}$,

$$\hat{M}_{\perp y}(Q_y, Q_z) = -\frac{Q_z}{Q^2}(Q_y\hat{M}_z - Q_z\hat{M}_y)\,, \quad \hat{M}_{\perp z}(Q_y, Q_z) = \frac{Q_y}{Q^2}(Q_y\hat{M}_z - Q_z\hat{M}_y)\,. \tag{5}$$

It is interesting to note that there exists an ambiguity when the scattering vector approaches forward scattering, $\mathbf{Q} \to 0$,

$$\begin{array}{rcl} \lim\limits_{Q_y \to 0} \langle b(Q_y, Q_z = 0)\rangle & = & b_c + b_m P_z \hat{M}_z \\ \lim\limits_{Q_z \to 0} \langle b(Q_y = 0, Q_z)\rangle & = & b_c + b_m P_y \hat{M}_y \end{array}\,. \tag{6}$$

In general the dimensions of the scatterers will be distributed which can be described by an appropriate size probability density function $P(\mathbf{a})$ which depends of on a set $\mathbf{a}$ of size parameters. Then, the scattered intensity has to be weighted accordingly,

$$I(\mathbf{Q}) \propto \langle|\rho(\mathbf{Q})|^2\rangle = \int (N\langle b(\mathbf{Q})\rangle V(\mathbf{a}))^2 S(\mathbf{Q}, \mathbf{a}) P(\mathbf{a}) \mathrm{d}^n\mathrm{a} \tag{7}$$

Examples for the set $\mathbf{a}$ are, e.g. the radius of a spherical scatterer $a_1 = R$ and the width of its distribution σ_R, a set with $n = 1$, or the correlation length a_1 along the ribbon axis and a_2 perpendicular to the ribbon axis, a set with $n = 2$ parameters. The intensity as given by eq. (7) is not directly accessible by USANSPOL measurements. Therefore, it is convenient to express this intensity as a conditional probability of scattering about $\mathbf{Q} = (Q_y, Q_z)$ given that scattering occurs at all,

$$P_{scat}(Q_y, Q_z) = P_{scat}(Q_y, Q_z|scattering) = \frac{1}{C_{yz}} \int (N\langle b(Q_y, Q_z)\rangle V(\mathbf{a}))^2 S(Q_y, Q_z, \mathbf{a}) P(\mathbf{a}) \mathrm{d}^n\mathrm{a} \tag{8}$$

where C_{yz} is the appropriate normalisation constant. Image plot (a) in Fig. 1 shows this probability density function resulting from a model calculation of stripe-like scatterers with dimensions a_y, a_z that are normal distributed about $a_{y0} = 5$ μm and $a_{z0} = 3.3$ μm with relative widths $\sigma_y/a_{y0} = \sigma_z/a_{z0} = 0.2$. In the image plots the colour scale representing $\log(P_{scat}(Q_y, Q_z))$ ranges from $10^{-1.5}$ (top yellow) to $10^{-8.5}$ (bottom black). A USANSPOL setup integrates the corresponding intensity along the Q_z axis which results in a 1-dim. dependence of Q_y,

$$P_{scat}(Q_y) = \frac{1}{C_N} \int \mathrm{d}Q_z \int \mathrm{d}^n\mathrm{a} (N[b_c + b_m(P_y\hat{M}_{\perp y}(Q_y, Q_z) + P_z\hat{M}_{\perp z}(Q_y, Q_z)]V(\mathbf{a}))^2 S(Q_y, Q_z, \mathbf{a}) P(\mathbf{a}) \tag{9}$$

with $C_N = \int \mathrm{d}Q_y P_{scat}(Q_y)$. This conditional probability is displayed as red curve in graph (d) of Fig. 1. It is quite clear from the mathematical structure of this integral that the micro-structure of such samples will not be revealed in a single measurement, except under simple model assumptions like form isotropy of the scatterers as it was applied in [1]. From our current point of view we expect that rotation of the sample and measurements at different angular positions will provide additional information for and constraints on the data analysis in a somewhat similar manner than in tomographic reconstruction. In our case, the respective orientation of the scattering vector, the sample magnetisation and the neutron polarisation is varied while the internal structure of the sample remains unchanged. This is illustrated in images (b) and (c) of Fig. 1. In (a) the scatterer was assumed to be contained in a ribbon with vertical axis and magnetisation and neutron polarisation parallel to the ribbon axis. In (b) the ribbon was rotated by $\theta = 45°$ into the diagonal direction, in (c) by $\theta = 90°$ into the horizontal direction, in both cases the magnetisation and neutron polarisation where kept parallel to the ribbons axis. While in (a) this direction was perpendicular to Q_y it is parallel in (c) and at an intermediate angle in (b). Slit height smearing of these probabilities is shown in graph (d) as green curve for the 45° case and as blue curve for the 90° case. The data for (a)–(c) where calculated with the same structure function $S(Q'_y(\theta), Q'_z(\theta), \mathbf{a})$ but evaluated at a rotated scattering vector $Q'_y(\theta) = Q_y\cos\theta + Q_z\sin\theta$, $Q'_z(\theta) = Q_z\cos\theta - Q_y\sin\theta$ to take advantage of the symmetry of the problem. This symmetry is clearly visible in the image plots (a)–(c) in Fig. 1 as it would be in a 2-dim. SANS detector but is completely

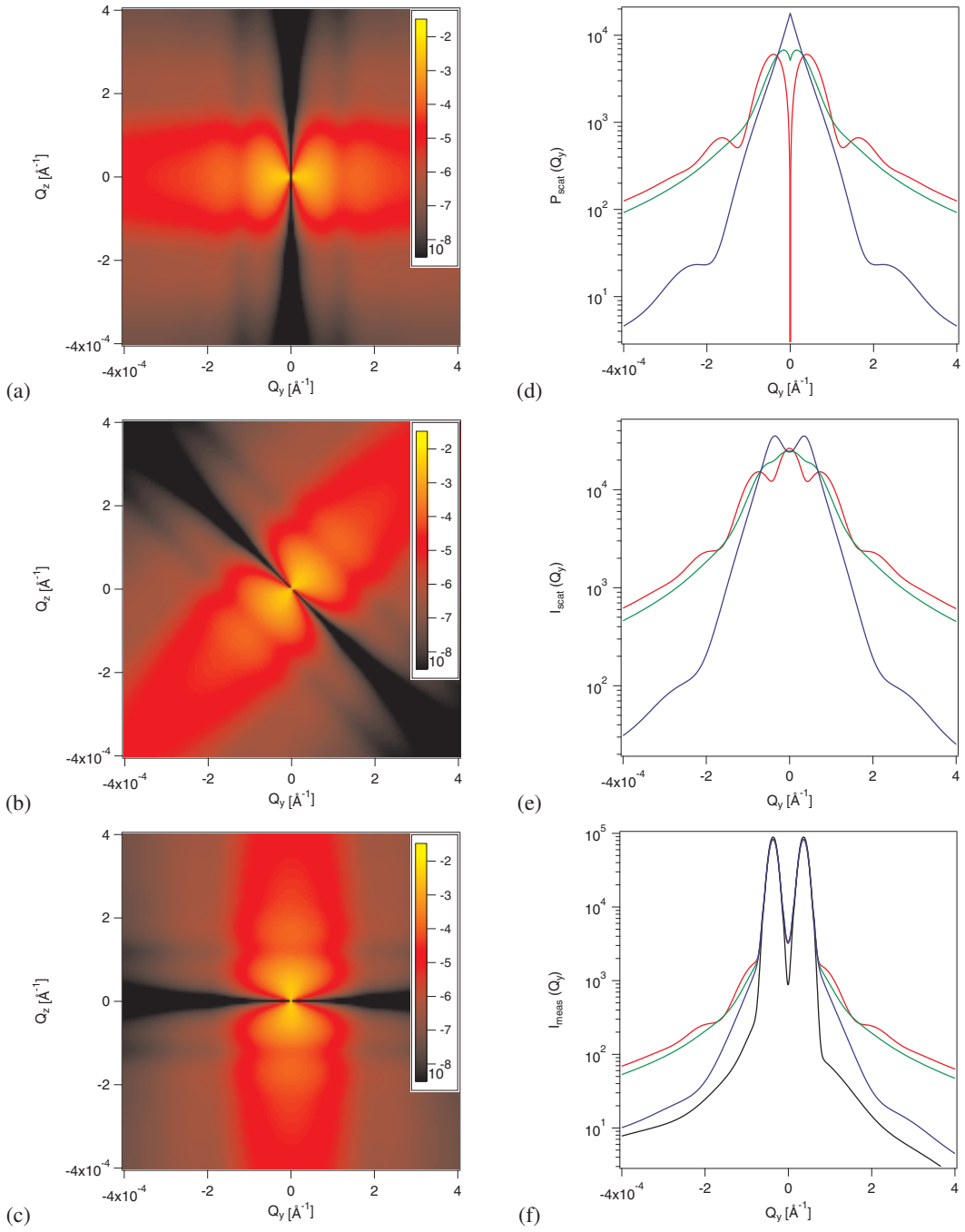

Fig. 1. Model calculations of stripe-like scatterers within a magnetic ribbon. The dimensions of the scatterers are normal-distributed with a mean size of 3.3 μm in direction of the ribbon axis and 5 μm in the perpendicular direction. The magnetisation and neutron polarisation were assumed parallel to the ribbon axis, also after rotation of the ribbon. Conditional probability for neutron scattering about the horizontal direction Q_y and the vertical direction Q_z given that scattering occurs: (a) ribbon axis oriented in vertical direction, $\theta = 0$, (b) ribbon oriented along the diagonal, $\theta = \pi/4$, (c) ribbon horizontal, $\theta = \pi/2$. The USANSPOL technique resolves Q_y scattering with high resolution only, intensity scattered in the vertical direction is integrated inherently: (d) conditional probability for scattering about Q_y given that scattering occurs. These curves result from integrating images (a) – (c) about Q_z for any given Q_y. This probability has to be convolved with the resolution function of the corresponding instrument, graph (e) shows the resulting scattered intensity after convolution of the curves in (d) with the specific resolution function of the instrument S18 at ILL, shown as black line in graph (f). A model of the actually measured intensity is shown in (f) assuming a scattering probability of 10%, background subtracted; the intensities in (e) and (f) are given as neutrons per minute. Graphs (d) – (f) display curves for the ribbon orientation $\theta = 0$: red, $\theta = \pi/4$: green, $\theta = \pi/2$: blue.

size distribution	$\int \mathrm{d}^n\mathrm{a}$
slit height smearing	$\int \mathrm{d}Q_z$
orientation averaging	$\int \mathrm{d}\theta$
normalisation	$\int \mathrm{d}Q_y$
convolution with the resolution function	$\int \mathrm{d}Q'$

Table 1. Summary of distribution, smearing and convolution integrations that lead to the measured USANSPOL neutron intensity.

lost in the slit height smeared curves of graph (d) where each additional angular position carries additional information for the structure analysis.

The curves in graph (d) of Fig. 1, however, represent an ideal limit for an infinitely narrow instrument resolution function. Real resolution functions were discussed and characterised in [1] and [2], and an example is shown as black line in graph (f) of Fig. 1. The scattered intensity is obtained by convolving the conditional probability for scattering $P_{scat}(Q_y)$ with the real instrument resolution function $R(Q_y)$ for both spin states of the incident neutron beam,

$$I_{\uparrow\downarrow scat}(Q_y) = \alpha_{\uparrow\downarrow} \int \mathrm{d}Q' R_{\uparrow\downarrow}(Q_y - Q') P_{\uparrow\downarrow scat}(Q_y) \tag{10}$$

where $\uparrow$ denotes the component of the neutron beam which is initially polarised in $+z$ direction and $\downarrow$ the component initially polarised in $-z$ direction. $\alpha_\uparrow$ and $\alpha_\downarrow$ are the total probabilities for spin up and spin down scattering and are treated currently as unknown parameters in our parameter estimation. Intensities calculated according to eq. (10) are shown in graph (e) of Fig. 1 where $\alpha_\uparrow = \alpha_\downarrow = 1$ to facilitate the comparison with graph (d). It will be noted that the intensity values, given in neutrons per minute in (e), depend on the incident neutron intensity, the similarity with the probability values in (d) which depend entirely on the structure is therefore purely accidental. The instrument resolution function used for the convolution is shown as black curve in graph (f) of Fig. 1 and was obtained at the instrument S18 at ILL, Grenoble. The colours of the curves in graph (e) indicate the angular position of the ribbon: red $\theta = 0$ (vertical), green $\theta = \pi/4$ (diagonal), and blue $\theta = \pi/2$ (horizontal), as in graph (d).

Finally, the measured intensity consists of the scattered intensity (10) with total scattering probabilities $\alpha_{\uparrow\downarrow} < 1$, an unscattered contribution $(1 - \alpha_{\uparrow\downarrow})R_{\uparrow\downarrow}(Q_y)$ and the instrument background I_B,

$$I_{meas}(Q_y) = I_{\uparrow scat}(Q_y) + I_{\downarrow scat}(Q_y) + (1 - \alpha_\uparrow)R_\uparrow(Q_y) + (1 - \alpha_\downarrow)R_\downarrow(Q_y) + I_B \,. \tag{11}$$

Graph (f) shows "measured intensities" from model calculations with $\alpha_\uparrow = \alpha_\downarrow = 0.1$ and the instrument resolution function as black curve. The colour code of the intensity curves correspond to the angular positions in graphs (d) and (e).

The task of the USANSPOL data analysis is summarised by the reverse sequence of the data shown in Fig. 1, specifically to start from the measured data as shown in graph (f) to arrive at the images shown in (a)–(c) where the inversion problem of SANS data begins. The mechanisms involved and discussed above are summarised in Tab. 1.

3. New experimental possibilities and exemplifying results

In order to realise the measurement scheme as suggested in the previous section, a dedicated sample environment has to be provided to adjust the angular orientation of the sample and the direction of neutron polarisation. Additionally, this sample environment has to provide for external parameters like magnetic field or mechanically induced stress. A first prototype of this kind was introduced in [2] and its design based on magnetic ribbon samples (see Fig. 4 in [2]). Experiences with this first prototype showed potential for improvement for the generation of weak external magnetic fields up to about 100 G. Magnetic fields of that strength are important to study the evolution of the magnetic microstructure in many modern magnetic materials, to align the polarization direction of the incoming neutron beam and to compensate unwanted

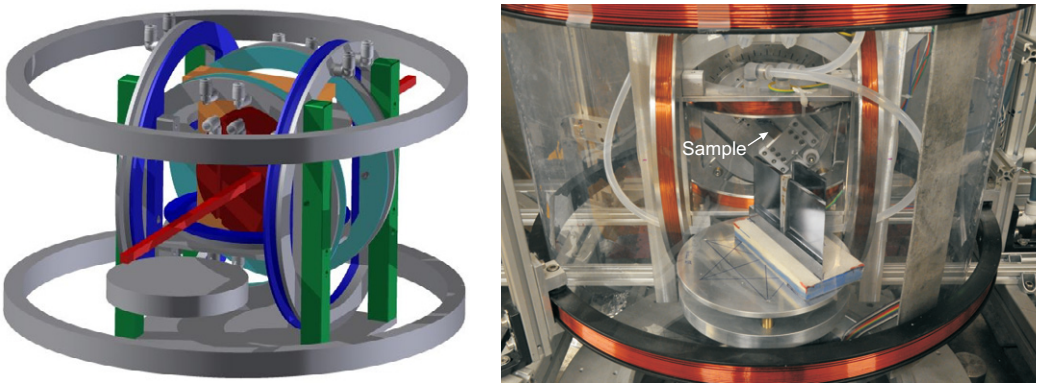

Fig. 2. 3D CAD sketch of the 3 Helmholtz coils (blue and turquoise) providing for an arbitrarily adjustable external magnetic field up to 100 G. The additional large Helmholtz coil which generates a magnetic field in vertical direction represents the standard magnetic environment at S18 and is mainly used as guide field for polarised neutron interferometry experiments. These coils are also used to define the neutron polarisation and to compensate unwanted environmental stray fields. The sample is placed on a rotating plate in the red plane at the centre of the Helmholtz coils. The photograph shows the actual installation of the USANSPOL sample environment, containing an amorphous magnetic ribbon, at S18 together with the channel-cut silicon analyser perfect crystal in the foreground.

environmental stray fields. The design consists of 3 orthogonal Helmholtz coils which allow for a 3-dim. control of the magnetic field at the sample position. The design of our improved prototype sample environment is shown in Fig. 2 together with its installation at the instrument S18 at ILL where it was placed inside the standard vertical neutron guide field produced by two large Helmholtz coils.

A certain limitation of the technique will be immediately apparent for our measurements. Since the external magnetic field influences the magnetisation of the sample as well as it defines the direction of neutron polarisation there will always be correlations between the corresponding quantitites in section 2.

Additional improvements of the sample environment concern the application of external mechanically induced stress. In the first prototype version this stress was produced by attaching containers of fixed weight to the ribbons, a concept which exerted stable forces on the ribbons but lacked a certain amount of flexibility and involved a steady risk for the analyser crystal axis. In our improved sample environment the force is generated by the torque of an electric motor with sufficient gear which is transferred via two elastic strings attached to both the motor axis and the ribbon under study. These two strings are connected via a force transducer which allows to monitor the applied force and to control it in a closed loop via computer software.

A selection of experimental results that may be obtained at a USANSPOL instrument with dedicated sample environment is shown in Fig. 3 for an $Fe_{78}Mo_2B_{20}$ ribbon. Blue curves show the ribbon in zero magnetic field with no external stress applied. Full symbols represent a vertical ribbon axis, open symbols a horizontal ribbon axis. These curves may be compared to the red and blue curve in graph (f) of Fig. 1. Although the difference is not as pronounced in the actual experiments the comparison suggests that both orientations have exchanged their effects on the scattering curves. This would imply a slightly larger extension of the domains along the ribbon axis and a preferred orientation of the magnetisation perpendicular to the ribbon axis in zero field environment. This trend then would increase with the application of an external magnetic field, the red curves in Fig. 3 which is plausible for the dimension of the domains along the ribbon axis but not for the magnetisation which would be enhanced perpendicular to the external magnetic field. These ambiguities illustrate the complex interplay of all the quantities discussed in section 2 and the necessity of a rigorous data treatment while the heuristic evaluation of the data faces severe limitations.

The application of mechanically induced stress without external magnetic field, the green curves in Fig. 3, leads to a pronounced enlargement of the domain size due to the magnetostriction properties of the material both parallel an perpendicular to the ribbon axis as can be concluded from the narrower scattering curves in both orientations. A combined application of stress and external magnetic field, the purple curves in Fig. 3, causes a similar change in the scattering as when moving from zero field conditions to external

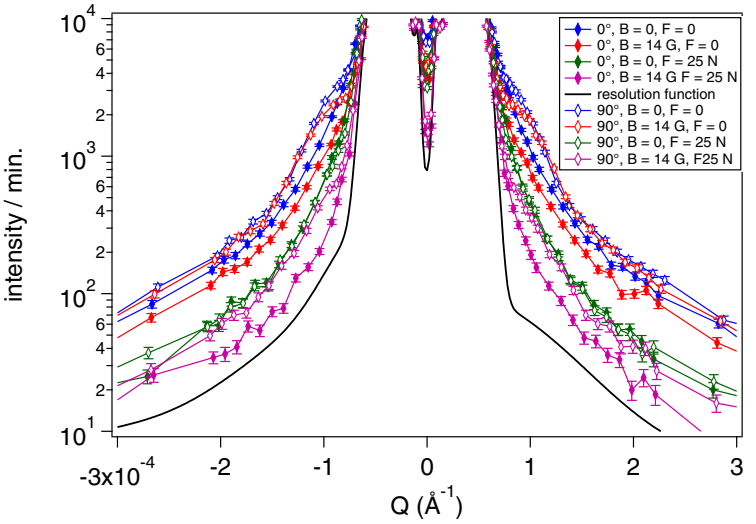

Fig. 3. USANSPOL intensities of an $Fe_{78}Mo_2B_{20}$ ribbon: full symbols represent a ribbon in vertical direction, open symbols in horizontal direction; blue and green curves were taken in magnetic zero field with $\mathbf{P} = P_z\hat{z} = \pm\hat{z}$, red and purple curves in an external magnetic field of 14 G – the field was applied in the direction of the ribbon axis and $\mathbf{P}$ parallel to $\mathbf{B}_{ext}$; blue and red curves without mechanically induced stress, green and purple curves with a mechanical stress of 39 MPa.

field in the unstressed ribbon, albeit now starting with larger domains.

It is important to note that the neutron polarisation remains parallel to the z axis in magnetic zero field for all orientations of the ribbon and that the polarisation vector is parallel to the external magnetic field which was applied parallel to the ribbon axis in all corresponding curves shown in Fig. 3. Also this fact further diminishes the feasibility of intuitive guesses of the magnetic microstructure from the phenomenology of the scattering curves.

In principle, USANSPOL measurement results allow an assessment of the native sample state which may exhibit form anisotropy due to a special manufacturing process. At the other end of the internal length scale, we can observe the sample under saturation conditions from which we may distinguish crystalline and amorphous states on a microstructure level with implications on the technological applicability of the material. The evolution of the magnetic structure between these two endpoints is seen from experiments with applied external magnetic field or mechanical stress of varying strength and can be followed up to the resolution limit of the technique where the scattering curves practically coincide with the instrument resolution function. Additional examples can again be found in references [1] and [2].

4. Conclusions and outlook

To conclude we can assert that USANSPOL is a potentially powerful technique for the study of magnetic microstructure of matter. However, data modelling and routine analysis are still in the developing phase - mainly owing to the formal complexity described in section 2. Technical development is also performed on the sample environment of the USANSPOL setup - an improved prototype version was recently tested and showed a variety of possibilities for the study of magnetic materials.

Acknowledgement

This project was supported by the European Integrated Infrastructure Initiative for Neutron Scattering and Muon Spectroscopy NMI3, FP7 Grant Agreement No. 226507-NMI3.

References

[1] E. Jericha, G. Badurek, R. Grössinger, Characterisation of novel magnetic materials using the usanspol technique, Physica B 406 (2011) 2401–2404.
[2] E. Jericha, C. G. G. Badurek, D. Süss, Experimental and methodic progress in ultra-small-angle polarised neutron scattering on novel magnetic materials, J. Phys. Conf. Ser. 340 (2012) 012007–1–12.